Combining sudomotor nerve impulse estimation with fMRI to investigate the central sympathetic response to nausea*

Roberta Sclocco, Luca Citi, *Member, IEEE,* Ronald G. Garcia, Sergio Cerutti, *Fellow, IEEE,* Anna M. Bianchi, *Member, IEEE,* Braden Kuo, Vitaly Napadow and Riccardo Barbieri, *Senior Member, IEEE*

Abstract— **The skin conductance (SC) signal is one of the most important non-invasive indirect measures of autonomic outflow. Several mathematical models have been proposed in the literature to characterize specific SC features. In this work, we present a method for the estimation of central control of sudomotor nerve impulse (SMI) function using SC. The method is based on a differential formulation decomposed into two first order differential equations. We validate our estimation framework by applying it on an experimental protocol where eleven motion sickness-prone subjects were exposed to a nauseogenic visual stimulus while SC and fMRI signals were recorded. Our results show an expected significant increase in the mean amplitude of SMI peaks during the highest reported nausea, as well as a decreasing trend during recovery, which was not evident for skin conductance level. Importantly, SMI/fMRI analysis found a negative association between SMI and fMRI signal in orbitofrontal, dorsolateral prefrontal, and posterior insula cortices, consistent with previous studies correlating brain fMRI and microneurographic signals.**

I. Introduction

Non-invasive neuroimaging techniques, and functional magnetic resonance imaging (fMRI) in particular, represent a powerful tool to reveal important information on the connection between high-level brain functions and physiology [1]. Specifically, the ability of recording peripheral autonomic signals concurrently with fMRI provides the possibility to evaluate the neural correlates of the autonomic nervous system (ANS), especially when investigating tasks or stimuli known to elicit robust autonomic response. Among the peripheral signals recorded to this purpose, skin conductance (SC) is one of the most widely used indirect measure of sympathetic activity [2]. Alterations in SC are determined by the eccrine sweat glands, which is innervated by the sympathetic branch of the ANS. SC can be recorded from different parts of the body, although the most responsive sweat glands are located on the palm of the hands. As a general feature, SC is constituted by two different components: a tonic component, called the skin conductance level (SCL) and suggested to be related to the overall level of arousal, and a phasic component, the skin conductance response (SCR), reflecting an evoked response to stimuli. For this latter component, a number of measures has been defined: SCR amplitude, latency, rise time, half recovery time and habituation parameters are often evaluated in order to characterize the sympathetic response [3]. The main limitation to this approach is represented by the overlap of consecutive SCRs when the inter-stimulus interval is shorter than the SCR recovery time (typically 10-20s). Thus, several studies have proposed solutions to provide a mathematical model of the phasic SC in order to separate individual SCRs [4]–[7]. The proposed models can be used in order to estimate the driver function generating the measured SC, and more closely reflecting the activity of the sudomotor nerve [5]. Such an approach offers the advantages of a non-invasive acquisition setup with respect to e.g. microneurography, as well as an easier acquisition setup. An additional advantage of being able to provide a better estimate of the dynamic characterization of the sympathetic nerve activity is that, when used in conjunction with fMRI, it can offer a more accurate mapping of the central autonomic network (CAN) during experimental protocols modulating autonomic outflow.

In this work, we present a method for the estimation of the sudomotor nerve impulse (SMI) function from skin conductance. The algorithm is then applied to real SC/fMRI data acquired from a study evaluating nausea in response to visual stimulation in susceptible individuals, to investigate the central sympathetic response to this aversive sensation.

*Research supported by Regione Lombardia and Fondazione Cariplo (THINK&GO project), by the Department of Anesthesia, Critical Care and Pain Medicine of the Massachusetts General Hospital and by the National Institutes of Health (NIH) with the following grants: R21-DK097499, S10-RR023043, S10-RR023401.

R. Sclocco is with the Department of Electronics, Information and Bioengineering, Politecnico di Milano, Italy (phone: +390223993322; e-mail: roberta.sclocco@polimi.it).

R. Sclocco, R.G. Garcia and V. Napadow are with A.A Martinos Center for Biomedical Imaging, Massachusetts General Hospital, Harvard Medical School, Boston, MA, USA (e-mails: roberta@nmr.mgh.harvard.edu; rgarcia@nmr.mgh.harvard.edu; vitaly@nmr.mgh.harvard.edu).

L. Citi is with School of Computer Science and Electronic Engineering, University of Essex, UK (e-mail: lciti@essex.ac.uk).

S. Cerutti and A.M. Bianchi are with the Department of Electronics, Information and Bioengineering, Politecnico di Milano, Italy (e-mails: sergio.cerutti@polimi.it; annamaria.bianchi@polimi.it).

B. Kuo is with the Gastroenterology Unit, Massachusetts General Hospital, Harvard Medical School, Boston, MA, USA (e-mail: bkuo@partners.org).

R. Barbieri is with Department of Anesthesia, Critical Care and Pain Medicine, Massachusetts General Hospital, Harvard Medical School, Boston, MA, USA (e-mail: barbieri@neurostat.mit.edu).

II. Materials and Methods

A. Subjects

Seventeen right-handed healthy female subjects (28.4±8.5 years) were included in the study after increased motion sickness susceptibility was assessed by a score of >60 on the Motion Sickness Susceptibility Questionnaire (MSSQ, [8]) and confirmed during a mock MRI behavioral session in which they reached a moderate level of nausea (>2 on a scale from 0 to 4, see below) when exposed to the nauseogenic stimulus. Informed consent was obtained from all participants, and the protocol was approved by the Human Research Committee of Massachusetts General Hospital.

B. Experimental Protocol

A nauseogenic visual stimulus was delivered to the subjects lying in a 1.5T Siemens Avanto MRI scanner by projecting it onto a concave screen covering both central and peripheral fields of view. The nausea sensation was induced by an alternation of black (1.2cm, 6.9° viewing angle) and white (1.85cm, 10.6° viewing angle) stripes linearly moving from left to right at 62.5°/sec. The subjects were asked to rate their nausea level through a button box on a scale ranging from "0" (no nausea) to "4" (severe nausea approaching vomiting). The stimulation, preceded and followed by a 5-minute fixation period, was stopped after 20 minutes or when subjects reached a nausea intensity level of 4.

C. Data Acquisition

Whole-brain blood oxygen level-dependent (BOLD) fMRI data were collected using a gradient echo T_2^*-weighted pulse sequence (TR/TE=3s/30ms, slice thickness=3.0mm, gap=0.6mm, matrix=64x64, FOV=200mm, FA=90°), continuously during the baseline, stimulus and recovery periods. Prior to the MRI session, MRI-compatible bipolar Ag/AgCl finger electrodes were placed on the palmar aspect of the second and fourth fingers of the left hand, allowing skin conductance monitoring during fMRI scanning (sampling frequency=400Hz) using Chart Data Acquisition Software on a laptop equipped with the Powerlab System (ADInstruments). Six out of the initial seventeen subjects showed a low-quality SC signal and were excluded from further analyses, which was therefore carried out on eleven subjects.

D. Data Analysis

BOLD data preprocessing steps were performed using FSL and included field map correction, brain extraction, motion correction, high-pass filtering (f>0.007Hz), spatial smoothing (FWHM=5mm) and normalization to MNI space.

In order to recover the sudomotor impulse function from the observed skin conductance, a deconvolution approach proposed by Alexander et al. (2005) was adopted. According to this model, the SMI function *q(t),* which represents the individual activation bursts of the sudomotor nerve, is related to the measured skin conductance *y(t)* through a differential equation:

$$(\tau_0\tau_1)\frac{d^2y}{dt^2} + (\tau_0 + \tau_1)\frac{dy}{dt} + y = q(t), \qquad (1)$$

where τ_0 and τ_1 are the time-constants governing the decaying tails and the rise time in the SC signal ($\tau_0 > \tau_1$). After decomposing a discrete-time version of (1) into two first-order differential equations, we derived *q(t)* using a cascade of two linear filters implementing a smoothed differentiation operator (Hann window with duration 6 s and 300 ms). The use of a smoothed derivative helps reduce unwanted out-of-band noise. Finally, the signal was lower-clipped to zero in order to remove non-physiologically plausible negative values.

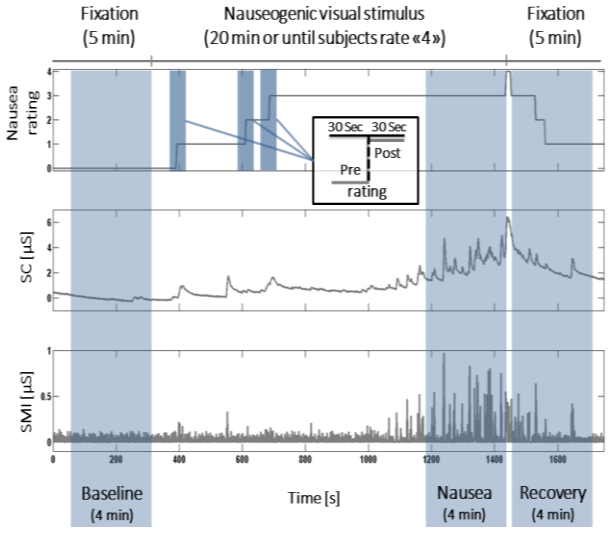

Figure 1. Schematic representation of experimental protocol design and data windowing for analysis. Nausea ratings, skin conductance and its sudomotor impulse function are shown from a representative subject.

As in our previous works [9], [10], we adopted two different approaches to define data windows for the analysis (see Fig. 1). In the first one, hereinafter referred to as protocol-driven analysis, 4-minute time windows were selected immediately before (BASELINE) and after (RECOVERY) the presentation of the stimulus, and a third window (NAUSEA) comprised the last 4 minutes of visual stimulation, when the most severe nausea sensation was experienced. The second approach, called rating-driven analysis, investigates the sympathetic response to increasing nausea sensation, selecting 1-minute time windows centered on individual nausea rating transitions (0to1, 1to2, 2to3) and looking at the difference between post- and pre-transition 30s periods. For each of the aforementioned time windows, two features of the sudomotor impulse function were considered, that is, the amplitude and the number of peaks. Since the hypothesis of Gaussianity of both features was rejected (Kolmogorov-Smirnov test, $p<0.05$), statistical analysis was performed through non-parametric tests. The two inter-subject analyses were carried out in order to investigate the features variations. In the protocol-driven analysis, statistical significance was assessed by a Friedman test followed by post-hoc pairwise comparisons (Bonferroni correction adopted, significance set at $p=0.05$); in

the rating-driven analysis, differences across the rating changes were assessed by means of Wilcoxon signed rank tests. Finally, the neural correlates of the sudomotor impulse function during nausea were investigated through an SMI/fMRI analysis. For this purpose, the individual sudomotor impulse functions were low-pass filtered at 0.33Hz, resampled at the fMRI sampling frequency, windowed within the NAUSEA period, and convolved with a gamma hemodynamic response function, in order to be used in the fMRI General Linear Model (GLM) analysis. The BOLD data were similarly windowed and single-subject and group analyses were carried out using FSL. All statistical brain maps were corrected for multiple comparisons ($Z>2.3$, $p<0.05$).

III. Results

Nine out of the eleven subject included in the analysis reached a level of "4" during the stimulation, while the other two subjects reported a maximum level of "3", thus indicating strong nausea sensation.

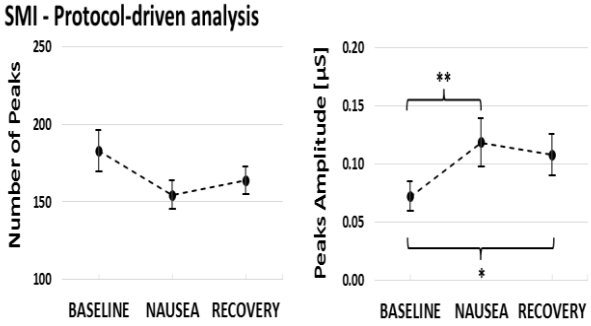

Figure 2. SMI number (left panel) and amplitude (right panel) of peaks (mean ± SEM) for the 4-minute windows (BASELINE, NAUSEA, RECOVERY). *(*p<0.05; **p<0.01)*

A. Sudomotor impulse function analysis

Results from the two protocol-based analysis of sudomotor impulse function are reported in Fig. 2. An overall significant effect of time window (BASELINE, NAUSEA and RECOVERY) was found only for the mean amplitude of SMI peaks. Post-hoc pairwise comparisons confirmed significant increase from BASELINE (amplitude of peaks: 0.07±0.01µS, mean ± SEM) in both NAUSEA (0.12±0.02µS, $p<0.01$) and RECOVERY (0.11±0.02µS, $p<0.05$) time windows. As for the number of peaks, a decrease from BASELINE (number of peaks: 182.82±13.41) was found in both NAUSEA (154.18±9.13) and RECOVERY (163.64±9.02) periods, but no significant effect was confirmed by Friedman test. The results of the rating-driven analysis did not show any significant difference during transition towards higher nausea levels for both the considered features. The mean post-pre variation in number of peaks did not reveal a particular pattern across transitions ("0to1": -0.18±1.02; "1to2": 0.36±1.56; "2to3": -0.44±2.16), while a decreasing trend was noticed when considering the amplitude of SMI peaks ("0to1": 0.007±0.010µS; "1to2": 0.003±0.015µS; "2to3": -0.005±0.30µS), suggesting an increase in the peaks amplitude in the 30 seconds preceding the transition as higher nausea sensations were reached.

B. SMI/fMRI analysis

The group map showing the neural correlates of SMI during NAUSEA time window is shown in Fig. 3. A negative relationship between fMRI signal and sudomotor impulse function was found in a diffuse network of brain regions encompassing putamen, orbitofrontal cortex (OFC), dorso-lateral prefrontal cortex (dlPFC), ventral middle/posterior insular cortex (vm/pIns) and extrastriate cortex consistent with MT+/V5. Other areas, showing a similar pattern, included bilateral fusiform gyri (FuG), para-hippocampus (PHG), primary and secondary somatosensory cortices (S1, S2), as well as cerebellum.

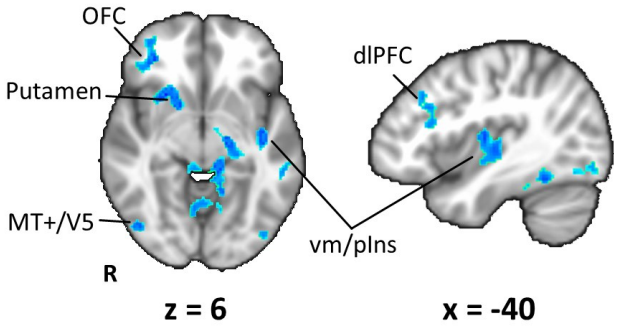

Figure 3. Group map (N=11) showing the neural correlates of the Sudomotor impulse response during NAUSEA time window. Significant negative correlation between BOLD and SMI signals ($Z>2.3$, $p<0.05$) is found in brain regions such as orbitofrontal and prefrontal cortices, putamen and middle/posterior insular cortex.

IV. Discussion

In this work, we proposed an estimation of the sudomotor impulse function from skin conductance measurements acquired during a visual nauseogenic stimulation. The sudomotor impulse function was recovered using a simple method based on a deconvolution approach but implemented as computationally inexpensive linear filters.

We analyzed the resulting time series adopting two different approaches for windowing data (Fig. 1), in order to test the ability of two SMI features (number and amplitude of peaks) aimed at estimating the sympathetic response to the stimulation. Results from the protocol-driven analysis (Fig. 2) showed a significant increase in the mean amplitude of SMI peaks during the last 4 minutes of visual stimulus (NAUSEA time window) and the first 4 minutes after the termination of the stimulus (RECOVERY time window). Interestingly, while our previous study analyzing the same dataset also showed an increase in SCL during NAUSEA, the RECOVERY period was associated with increased SCL, while the SMI shows a decreasing trend. At the same time, parasympathetic response as measured by the high-frequency component of heart rate variability (HF-HRV) showed the

highest decrease with respect to BASELINE during the NAUSEA time window, which rebounded toward baseline levels during RECOVERY [10]. Taken together, these results suggest a faster response for SMI compared with SCL, which is known to be an indirect and delayed measure of sympathetic activity [11]. As for the rating-driven analysis, none of the transitions towards higher nausea levels showed a significant change in SMI number or amplitude of peaks, though SCL had been found responsive in our previous results. A possible explanation could be the choice of the time windows for the rating-driven analysis: 30-second segments centered on the transition time may not be optimal for SMI, as this index may reflect faster dynamics in autonomic signaling, similar to HF-HRV.

Finally, we used the SMI signal as a regressor of interest in fMRI GLM analysis, in order to identify the neural correlates of the sympathetic outflow within the NAUSEA time window, when the highest nausea sensation was experienced by the subjects. The nausea state is ideal for ANS/fMRI analysis, since this sensation is known to elicit robust affective response and ANS outflow [12], [13]. Our previous studies showed the involvement of both sympathetic and parasympathetic branches of ANS [9], as well as some sympathetic/parasympathetic specificity in the underlying brain circuitry [10], where SCL was adopted as a measure of sympathetic activity. The SMI/fMRI group analysis presented here (Fig. 3) shows a negative relationship between BOLD signal and SMI in a network of cortical and subcortical brain regions. Interestingly, recent studies combining fMRI with concurrent recording of skin sympathetic nerve activity (SSNA) during emotional arousal have shown a negative relationship between SSNA and BOLD in areas such as OFC, dlPFC and posterior insula [14], [15], consistent with our results for SMI and nausea. Furthermore, right orbitofrontal cortex has been suggested as a key region for central control of electrodermal responses to emotional stimuli [16], consistent with our results. Furthermore, several of these areas (i.e. insula, putamen, OFC, dlPFC) also demonstrated tonic activation in response to increasing nausea in our previous study [17], and our current results thus suggest the specific regions of the general brain response to nausea, that are associated with sympathetic response to motion sickness.

V. Conclusions

In the present work, we suggest that estimation of the underlying sudomotor impulse function from peripheral skin conductance signal might represent a valid alternative to invasive sympathetic measurements (e.g. microneurography). Physiological monitoring for SMI is possible with concurrent magnetic resonance imaging, allowing for applications such as the investigation of central autonomic control of sympathetic outflow in response to motion sickness.

References

[1] V. Iacovella and U. Hasson, "The relationship between BOLD signal and autonomic nervous system functions: implications for processing of 'physiological noise,'" *Magn. Reson. Imaging*, vol. 29, no. 10, pp. 1338–1345, Dec. 2011.

[2] S. D. Kreibig, "Autonomic nervous system activity in emotion: A review," *Biol. Psychol.*, vol. 84, no. 3, pp. 394–421, Jul. 2010.

[3] M. E. Dawson, A. M. Schell, and D. L. Filion, "The electrodermal system," in *Handbook of psychophysiology (3rd ed.)*, J. T. Cacioppo, L. G. Tassinary, and G. G. Berntson, Eds. New York, NY, US: Cambridge University Press, 2007, pp. 159–181.

[4] C. L. Lim, C. Rennie, R. J. Barry, H. Bahramali, I. Lazzaro, B. Manor, and E. Gordon, "Decomposing skin conductance into tonic and phasic components," *Int. J. Psychophysiol.*, vol. 25, no. 2, pp. 97–109, Feb. 1997.

[5] D. M. Alexander, C. Trengove, P. Johnston, T. Cooper, J. P. August, and E. Gordon, "Separating individual skin conductance responses in a short interstimulus-interval paradigm," *J. Neurosci. Methods*, vol. 146, no. 1, pp. 116–123, Jul. 2005.

[6] D. R. Bach, G. Flandin, K. J. Friston, and R. J. Dolan, "Time-series analysis for rapid event-related skin conductance responses," *J. Neurosci. Methods*, vol. 184, no. 2, pp. 224–234, Nov. 2009.

[7] A. Greco, A. Lanata, G. Valenza, E. P. Scilingo, and L. Citi, "Electrodermal activity processing: A convex optimization approach," in *2014 36th Annual International Conference of the IEEE Engineering in Medicine and Biology Society (EMBC)*, 2014, pp. 2290–2293.

[8] J. F. Golding, "Motion sickness susceptibility questionnaire revised and its relationship to other forms of sickness," *Brain Res. Bull.*, vol. 47, no. 5, pp. 507–516, Nov. 1998.

[9] L. T. LaCount, R. Barbieri, K. Park, J. Kim, E. N. Brown, B. Kuo, and V. Napadow, "Static and Dynamic Autonomic Response with Increasing Nausea Perception," *Aviat. Space Environ. Med.*, vol. 82, no. 4, pp. 424–433, Apr. 2011.

[10] R. Sclocco, J. Kim, R. G. Garcia, J. D. Sheehan, F. Beissner, A. M. Bianchi, S. Cerutti, B. Kuo, R. Barbieri, and V. Napadow, "Brain Circuitry Supporting Multi-Organ Autonomic Outflow in Response to Nausea," *Cereb. Cortex*, p. bhu172, Aug. 2014.

[11] W. Boucsein, *Electrodermal Activity*. Springer Science & Business Media, 2012.

[12] E. R. Muth, "Motion and space sickness: Intestinal and autonomic correlates," *Auton. Neurosci.*, vol. 129, no. 1–2, pp. 58–66, Oct. 2006.

[13] S. Ohyama, S. Nishiike, H. Watanabe, K. Matsuoka, H. Akizuki, N. Takeda, and T. Harada, "Autonomic responses during motion sickness induced by virtual reality," *Auris. Nasus. Larynx*, vol. 34, no. 3, pp. 303–306, Sep. 2007.

[14] L. A. Henderson, A. Stathis, C. James, R. Brown, S. McDonald, and V. G. Macefield, "Real-time imaging of cortical areas involved in the generation of increases in skin sympathetic nerve activity when viewing emotionally charged images," *NeuroImage*, vol. 62, no. 1, pp. 30–40, Aug. 2012.

[15] V. G. Macefield, C. James, and L. A. Henderson, "Identification of sites of sympathetic outflow at rest and during emotional arousal: Concurrent recordings of sympathetic nerve activity and fMRI of the brain," *Int. J. Psychophysiol.*, vol. 89, no. 3, pp. 451–459, Sep. 2013.

[16] H. D. Critchley, R. Elliott, C. J. Mathias, and R. J. Dolan, "Neural Activity Relating to Generation and Representation of Galvanic Skin Conductance Responses: A Functional Magnetic Resonance Imaging Study," *J. Neurosci.*, vol. 20, no. 8, pp. 3033–3040, Apr. 2000.

[17] V. Napadow, J. D. Sheehan, J. Kim, L. T. LaCount, K. Park, T. J. Kaptchuk, B. R. Rosen, and B. Kuo, "The Brain Circuitry Underlying the Temporal Evolution of Nausea in Humans," *Cereb. Cortex*, vol. 23, no. 4, pp. 806–813, Apr. 2013.